

Theoretical Studies on the Gas-Phase Wolff Rearrangement of Ketocarbenes

Chan Kyung Kim and Ikchoon Lee*

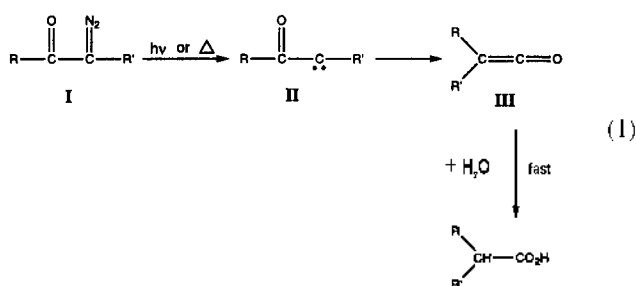
Department of Chemistry, Inha University, Incheon 402-751, Korea

Received January 21, 1997

The substituent effects in the gas-phase rearrangement of carbenes to ketenes involved in the Wolff reaction have been investigated theoretically using the AM1 method. In the initial state, carbene, there is a relatively strong vicinal $n-\sigma^*$ interaction between the lone pair (n) and carbonyl group (σ^*). In the bridged transition state (TS), electronic charge is transferred from the migrating ring (Z-ring) toward the nonmigrating ring (Y-ring). The carbenes are stabilized by an electron donor Y ($\delta\sigma_Y < 0$) whereas the TS is stabilized by an electron acceptor Y ($\delta\sigma_Y > 0$). Multiple regression analysis of $\log(k_{yz}/k_{zz}) (= -\delta\Delta G^\ddagger/2.3RT)$ leads to a relatively large negative cross-interaction constant, $\rho_{yz} = -0.53$, $\log(k_{yz}/k_{yy}) = 2.96\sigma_Y + 1.40\sigma_Z - 0.53\sigma_Y\sigma_Z$ reflecting an extensive structural change in the transition state due to the stabilization of the initial state by the vicinal $n-\sigma^*$ overlap. When the solvent (water) effects are accounted for by the SM2, 1 model of the Cramer and Truhlar method, the magnitude of all the selectivity parameters, ρ_Y , ρ_Z and ρ_{YZ} ($= -0.66$) are increased.

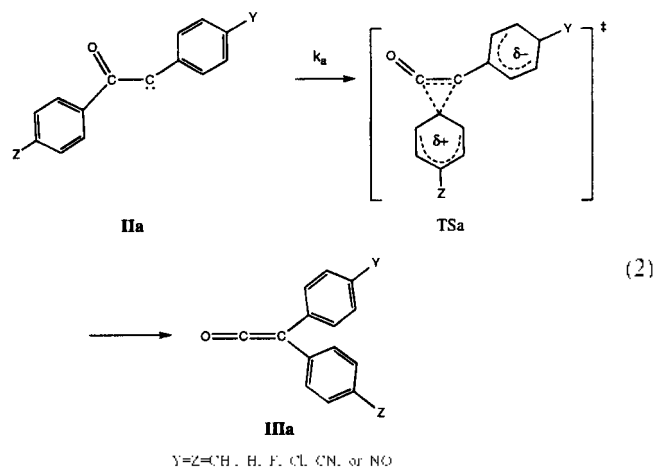
Introduction

L. Wolff¹ isolated products formed by rearrangement of the carbon skeleton in decomposing dicarbonyl diazo compounds in aqueous solution, (I). The products were rationalized by assuming a ketene intermediate, III.



Azibenzil ($R=R'=\text{Ph}$ in I) in MeOH at 50 °C afforded 70% of the Wolff rearrangement product, methyl diphenylacetate.² Elevated temperatures favor the Wolff rearrangement, and photolysis leads often successful "normal" rearrangement when other methods failed. Although the Wolff reaction may give a variety of final products, all of them can be derived from the intermediate ketene, III.¹ Thus, mechanistically the rearrangement process from singlet carbene, II, to ketene, III, is the most important step. In this work, effects of substituents in the two phenyl groups of azibenzil on the mechanism of the Wolff rearrangement in the gas phase, eq. 2, are examined.

For a disubstituted reaction system, we have been advocating nonadditivity of the substituent effects on the rate due to a cross-interaction term, ρ_{YZ} , in eq. 3.⁴ This simple second-order expression is obtained by a Taylor series expansion of $\log k_{YZ}$ around $\sigma_Y = \sigma_Z = 0$ with neglect of pure second-order (ρ_{YY} and ρ_{ZZ}) and higher-order (ρ_{YYZ} etc) terms. The cross-interaction constant, ρ_{YZ} , can be alter-



$$\log(k_{yz}/k_{zz}) = \rho_Y\sigma_Y + \rho_Z\sigma_Z - \rho_{YZ}\sigma_Y\sigma_Z \quad (3)$$

natively given by eq. 4, and is considered to represent a

$$\rho_{XY} = \frac{\partial \rho_Z}{\partial \sigma_Y} = \frac{\partial \rho_Y}{\partial \sigma_Z} \quad (4)$$

change in the intensity of interaction, ΔI_{YZ} , between the two substituents on going from the initial, I_{YZ}^* , to the transition state, I_{YZ}^\ddagger , eq. 5.^{5,6} The magnitude of ρ_{YZ} can therefore be

$$\rho_{YZ} \propto \Delta I_{YZ} = I_{YZ}^\ddagger - I_{YZ}^* \quad (5)$$

small when the two substituents interact strongly in the initial state as well as in the transition state (TS). The Wolff rearrangement is just such an example in which the migrating phenyl ring is initially (in carbene) bound by covalent bonds (strong interaction) but is partially cleaved in the TS with the two rings approaching nearer and interacting through dual routes (also strong interaction).

Calculations

The RIIF/AM1 method⁷ was used throughout in this

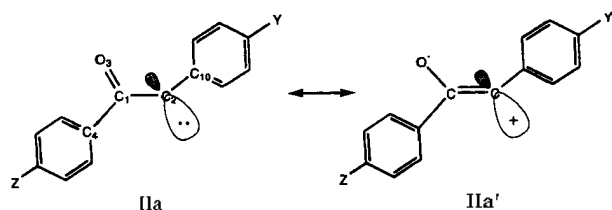
*To whom correspondence should be addressed.

work since the reactant, singlet carbenes, TS's and products have closed shell electron configurations. Geometries of all species were fully optimized and all stationary points were characterized by calculating the force-constant matrix and confirming all positive and only one negative eigenvalue for carbene and TS,⁸ respectively. Entropies (*S*) were calculated to arrive at Gibbs free energies (*G*), at *T*=298 K, *G*=*H*-*TS*. The solvent (water) effects were accounted for by use of SM2.1 model of the Cramer and Truhlar method.⁹ The free energy of solvation, ΔG_s , calculated by this method is the difference between the gas-phase and the aqueous-phase free energies. Since in this model the SCF results are parametrized using experimental data, they implicitly include electron correlation and configuration mixing effects¹⁰ just as AM1 does for the gas-phase solute energies.

Results and Discussion

Structures

Carbenes (IIa). The structure of the singlet carbene, IIa, is shown in Figure 1. The lone pair orbital on C₂ overlaps with the σ antibonding orbital of the vicinal carbonyl



group, $\sigma^*_{C_1-O}$ (*n*- σ^* interaction).¹¹ This elongates the C=O bond (1.25 Å vs 1.22 Å for the average of ketones¹²) but shortens the C₁-C₂ bond (1.42 Å vs 1.51 Å for the average value¹²). In addition, an electron donor *para*-substituent in the Y-ring, $\delta\sigma_Y < 0$ (e.g. Y=CH₃), intensifies this *n*- σ^* interaction, and the distance between C₂ and C₁₀, R_{2,10}, becomes contracted as a result of conjugative electron donation from Y toward C₁ (1.388 Å with Y=CH₃ and 1.406 Å with Y=NO₂ for Z=H). As a result, the carbene, IIa, is stabilized (*vide infra*). In fact the carbene is considered to form a resonance hybrid of IIa and IIa'. The bond distance

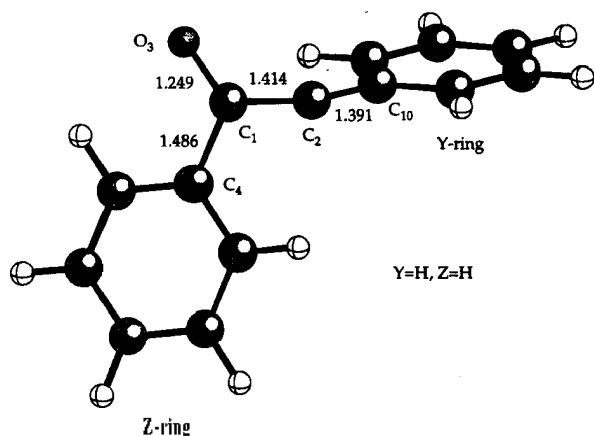
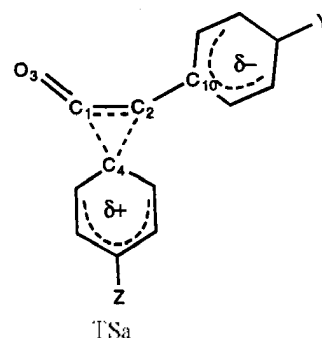


Figure 1. Structure of reactant (R). Y: H, Z: H. Bond lengths in Å.

data in Table 1 reveal that the two extremes of these structural effects are found with substituent combinations of Y=CH₃; Z=NO₂ (strongest effect) and Y=NO₂; Z=CH₃ (weakest effect); thus R_{1,2} and R_{2,10} are the shortest and the carbene is the more stable for the former, Y=CH₃; Z=NO₂ ($\Delta H_s = 97.00$ and 102.23 kcal mol⁻¹, respectively). In agreement with the resonance hybrid structure between IIa and IIa' due to the strongest *n*- σ^* interaction between the lone pair and $\sigma^*_{C_1-O}$ for the electron donor Y, $\delta\sigma_Y < 0$, the formal negative charge on O is larger (Table 2); $q_s = -0.345$ and -0.326 , respectively, with Y=CH₃ and Y=NO₂ for Z=H. Charge distribution of the two rings in Table 2 reveals that in general the Z-ring is negative whereas the Y-ring is positive: the stronger the *n*- σ^* interaction, the more negative is the Z-ring, the more positive is the Y-ring and the greater is the stability of the carbene (*vide infra*) due to the reso-



nance, IIa \leftrightarrow IIa'.

Transition states. The structure of the TS, TSa, is given in Figure 2. In the bridged TS structure, TSa, a partial double bond is formed between C₁ and C₂ with contraction of bond length of the bond C₁-C₂ and also C₁=O₃ (Table 1). These two bond contractions attending destruction of *n*- σ^* interaction in the TS cause electronic charge flow from the Z-ring toward the Y-ring (Table 2). Thus the TSa becomes more stabilized by a stronger electron donor Z ($\delta\sigma_Z < 0$) and by a strong electron acceptor Y ($\delta\sigma_Y > 0$). In fact the relative order of stability becomes inverted on going from the carbene (IIa) to the TS: now bond length of the two bonds, C₁-C₂ and C₂-C₁₀, are the shortest and the TSa is the most stable for Y=NO₂; Z=CH₃.

Ketenes. The structure of the ketene is presented in Figure 3.

Energetics

Heats of formation (ΔH_f), entropies (*S*), activation and reaction parameters, ΔG^\ddagger and ΔG^\ddagger , are summarized in Table 3. In general, a stronger donor Z ($\delta\sigma_Z < 0$) and a stronger acceptor Y ($\delta\sigma_Y > 0$) destabilize the reactant, carbene (IIa), more ($\delta\Delta H_f > 0$), but stabilize the TS (TSa) more ($\delta\Delta H_f^\ddagger < 0$) leading to a lower activation barrier, $\delta\Delta G^\ddagger < 0$. This means that there is a relatively large structural change on going from the reactant, carbene IIa, to the TS.

In contrast, however, both stronger acceptors Z ($\delta\sigma_Z > 0$) and Y ($\delta\sigma_Y > 0$) stabilize the product, ketene, more leading to a greater exothermicity of the reaction, $\delta\Delta G < 0$. Thus for a fixed Z, a stronger acceptor Y ($\delta\sigma_Y > 0$) leads to a greater exothermicity ($\delta\Delta G < 0$) as well as a lower activation barrier

Table 1. AM1 optimized bond lengths of reactant, TS, and product in Å

Z	Y	Reactant					TS					Product				
		C ₁ -C ₂	C ₁ -O ₃	C ₁ -C ₄	C ₂ -C ₄	C ₂ -C ₁₀	C ₁ -C ₂	C ₁ -O ₃	C ₁ -C ₄	C ₂ -C ₄	C ₂ -C ₁₀	C ₁ -C ₂	C ₁ -O ₃	C ₁ -C ₄	C ₂ -C ₄	C ₂ -C ₁₀
CH ₃	CH ₃	1.413	1.250	1.485	2.438	1.388	1.329	1.221	1.607	1.842	1.403	1.333	1.188	2.410	1.459	1.459
	H	1.414	1.249	1.485	2.438	1.392	1.329	1.221	1.605	1.845	1.403	1.333	1.188	2.410	1.459	1.459
	F	1.415	1.249	1.485	2.439	1.390	1.330	1.220	1.603	1.843	1.401	1.333	1.187	2.409	1.459	1.458
	Cl	1.416	1.249	1.484	2.439	1.393	1.329	1.221	1.598	1.849	1.400	1.333	1.187	2.409	1.460	1.457
	CN	1.420	1.248	1.483	2.440	1.399	1.323	1.221	1.583	1.861	1.388	1.334	1.186	2.407	1.461	1.455
	NO ₂	1.425	1.247	1.482	2.442	1.406	1.327	1.220	1.576	1.860	1.384	1.335	1.185	2.406	1.463	1.452
H	CH ₃	1.412	1.250	1.486	2.438	1.388	1.329	1.220	1.615	1.844	1.403	1.333	1.188	2.410	1.459	1.459
	H	1.414	1.249	1.486	2.438	1.391	1.329	1.220	1.613	1.847	1.403	1.333	1.188	2.410	1.459	1.459
	F	1.414	1.249	1.485	2.439	1.389	1.329	1.220	1.611	1.845	1.402	1.333	1.187	2.410	1.459	1.458
	Cl	1.415	1.249	1.485	2.439	1.392	1.329	1.220	1.607	1.850	1.401	1.333	1.187	2.410	1.460	1.458
	CN	1.413	1.248	1.484	2.440	1.399	1.321	1.220	1.591	1.863	1.389	1.334	1.186	2.408	1.461	1.455
	NO ₂	1.424	1.247	1.483	2.442	1.406	1.325	1.219	1.584	1.861	1.385	1.335	1.185	2.406	1.463	1.452
F	CH ₃	1.411	1.250	1.486	2.437	1.387	1.330	1.220	1.622	1.840	1.403	1.333	1.187	2.411	1.458	1.459
	H	1.413	1.249	1.486	2.438	1.390	1.330	1.220	1.610	1.844	1.404	1.333	1.187	2.411	1.458	1.459
	F	1.413	1.249	1.485	2.438	1.388	1.331	1.219	1.608	1.842	1.402	1.333	1.187	2.411	1.458	1.459
	Cl	1.414	1.249	1.485	2.439	1.391	1.331	1.220	1.604	1.847	1.402	1.333	1.187	2.410	1.459	1.458
	CN	1.418	1.248	1.484	2.440	1.397	1.323	1.220	1.587	1.862	1.390	1.334	1.186	2.409	1.460	1.456
	NO ₂	1.423	1.247	1.483	2.441	1.404	1.326	1.219	1.580	1.860	1.385	1.335	1.185	2.407	1.462	1.452
Cl	CH ₃	1.410	1.250	1.487	2.437	1.386	1.330	1.219	1.619	1.843	1.404	1.333	1.187	2.411	1.457	1.460
	H	1.412	1.249	1.487	2.437	1.390	1.330	1.219	1.617	1.846	1.404	1.333	1.187	2.411	1.458	1.460
	F	1.412	1.249	1.486	2.438	1.387	1.330	1.219	1.615	1.844	1.403	1.333	1.187	2.412	1.458	1.459
	Cl	1.414	1.249	1.486	2.438	1.390	1.330	1.219	1.611	1.849	1.403	1.334	1.187	2.411	1.458	1.459
	CN	1.418	1.248	1.485	2.439	1.397	1.322	1.220	1.594	1.864	1.390	1.334	1.186	2.409	1.460	1.456
	NO ₂	1.422	1.247	1.484	2.441	1.404	1.325	1.219	1.585	1.862	1.385	1.335	1.185	2.407	1.462	1.453
CN	CH ₃	1.408	1.249	1.489	2.435	1.384	1.329	1.218	1.636	1.849	1.405	1.334	1.186	2.413	1.455	1.461
	H	1.410	1.249	1.488	2.436	1.387	1.321	1.218	1.632	1.851	1.405	1.334	1.186	2.413	1.455	1.461
	F	1.410	1.249	1.488	2.437	1.385	1.329	1.218	1.631	1.849	1.404	1.334	1.186	2.413	1.456	1.460
	Cl	1.411	1.249	1.488	2.437	1.388	1.330	1.218	1.627	1.853	1.404	1.334	1.186	2.412	1.456	1.460
	CN	1.415	1.248	1.487	2.439	1.395	1.327	1.218	1.614	1.863	1.399	1.335	1.185	2.411	1.458	1.458
	NO ₂	1.420	1.247	1.486	2.440	1.402	1.321	1.218	1.601	1.868	1.386	1.336	1.184	2.409	1.460	1.455
NO ₂	CH ₃	1.404	1.249	1.491	2.434	1.380	1.330	1.216	1.654	1.859	1.405	1.335	1.185	2.416	1.452	1.464
	H	1.406	1.249	1.491	2.435	1.384	1.330	1.216	1.652	1.861	1.406	1.335	1.185	2.415	1.452	1.463
	F	1.406	1.249	1.490	2.436	1.381	1.330	1.216	1.651	1.859	1.404	1.335	1.185	2.417	1.452	1.463
	Cl	1.407	1.248	1.490	2.436	1.385	1.330	1.216	1.648	1.862	1.405	1.335	1.185	2.415	1.452	1.462
	CN	1.412	1.247	1.490	2.438	1.392	1.330	1.216	1.637	1.868	1.404	1.336	1.184	2.413	1.454	1.460
	NO ₂	1.416	1.246	1.488	2.440	1.399	1.317	1.216	1.621	1.879	1.389	1.337	1.183	2.411	1.456	1.457

($\delta\Delta G^\ddagger < 0$), but for a fixed Y a stronger acceptor Z ($\delta\sigma > 0$) leads to a greater exothermicity ($\delta\Delta G^\circ < 0$) but to a higher activation barrier ($\delta\Delta G^\ddagger > 0$).

These energetic are in agreement with the results of substituent effects on the stabilities of the carbene, TS and ketene: the reactant is stabilized by the vicinal $n_{C_2}-\sigma^*_{C_1}$ overlap whereas the TS is stabilized by the efficient electronic charge flow from the Z-ring toward the Y-ring. The ketene is obviously stabilized by lowering electronic charge from the ketene moiety, $-C=C=O$.

Cross-Interaction Constant ρ_{yz}

The ΔG^\ddagger values in Table 3 are used to calculate the Hammett's ρ values by eq. 6. Since in the Y-ring relatively

$$\delta \log k_a = -\frac{1}{2.3RT} \delta \Delta G^\ddagger = \rho \sigma \quad (6)$$

strong negative charge develops, the use¹⁹ of σ^- rather than

the normal σ improved the linear correlation substantially. We therefore used the σ^- constant for the substituent in the Y-ring. (σ^-_y). The results are collected in Table 4. As predicted from the formal charges in Table 2, ρ_z is negative and ρ_y is positive indicating that electronic charge is lost from the Z-ring (positive charge develops) whereas it is gained in the Y-ring (negative charge develops) on going from the carbene to the TSa. Again the positive charge developed in the TS at C₁ is stabilized or partially neutralized by an electron donor Z (a less negative ρ_z), while the negative charge developed in the TS on C₂ is stabilized by an electron acceptor Y (a less positive ρ_y).

Multiple regression of ΔG^\ddagger (eq. 6) using eq. 3 gave the cross-interaction constant, $\rho_{yz} = -0.53$, as expressed by eq. 7. It is instructive to compare this expression, eq. 7, with

$$\log(k_{cat}/k_{non}) = 2.96\sigma_1 - 1.40\sigma_2 - 0.53\sigma_1\sigma_2 \quad (7)$$

the corresponding one for the base-catalyzed rearrangement

Table 2. Formal charges (q_i) of reactant (R) and changes in formal charges, $\Delta q^*(q_i' - q_i)$, and $\Delta q(q_i - q_i)$ in electronic charge unit

Z	Y	q_i						Δq^*			Δq					
		C ₁	C ₂	O	Z-ring	Y-ring	C ₁₀	C	O	Z-ring	Y-ring	C	C	O	Z-ring	Y-ring
CII	CH	0.268	-0.113	-0.350	-0.013	0.209	0.069	-0.080	0.056	0.045	-0.090	0.011	-0.094	0.215	0.045	-0.177
	H	0.265	-0.105	-0.346	-0.010	0.196	0.074	-0.089	0.054	0.046	-0.085	0.014	-0.104	0.213	0.043	-0.166
	F	0.267	-0.109	-0.345	-0.008	0.195	0.075	-0.092	0.055	0.049	-0.087	0.014	-0.100	0.215	0.045	-0.173
	Cl	0.265	-0.102	-0.343	-0.007	0.187	0.082	-0.098	0.055	0.056	-0.094	0.018	-0.110	0.214	0.044	-0.167
	CN	0.259	-0.084	-0.336	-0.001	0.162	0.118	-0.128	0.056	0.087	-0.134	0.031	-0.134	0.212	0.045	-0.155
	NO	0.255	-0.061	-0.327	0.009	0.124	0.129	-0.155	0.060	0.095	-0.128	0.046	-0.165	0.212	0.046	-0.139
II	CH	0.267	-0.114	-0.349	-0.015	0.211	0.068	-0.075	0.058	0.036	-0.087	0.012	-0.095	0.215	0.046	-0.179
	H	0.265	-0.106	-0.345	-0.013	0.199	0.072	-0.084	0.056	0.037	-0.082	0.016	-0.105	0.213	0.044	-0.168
	F	0.266	-0.110	-0.344	-0.010	0.198	0.073	-0.087	0.057	0.040	-0.084	0.015	-0.100	0.215	0.045	-0.175
	Cl	0.264	-0.103	-0.342	-0.009	0.190	0.078	-0.091	0.057	0.045	-0.089	0.020	-0.110	0.214	0.045	-0.168
	CN	0.259	-0.085	-0.334	-0.003	0.164	0.117	-0.123	0.059	0.078	-0.131	0.032	-0.134	0.212	0.046	-0.156
	NO	0.254	-0.064	-0.326	0.006	0.130	0.129	-0.149	0.062	0.086	-0.127	0.047	-0.164	0.212	0.047	-0.143
F	CH	0.270	-0.118	-0.348	-0.024	0.220	0.065	-0.069	0.060	0.035	-0.090	0.010	-0.091	0.218	0.046	-0.184
	H	0.267	-0.109	-0.345	-0.021	0.207	0.069	-0.079	0.057	0.037	-0.084	0.014	-0.102	0.216	0.044	-0.172
	F	0.269	-0.114	-0.343	-0.019	0.206	0.070	-0.081	0.059	0.039	-0.087	0.013	-0.097	0.218	0.045	-0.179
	Cl	0.270	-0.106	-0.341	-0.017	0.198	0.074	-0.086	0.058	0.044	-0.090	0.018	-0.107	0.217	0.046	-0.173
	CN	0.261	-0.088	-0.334	-0.012	0.172	0.112	-0.116	0.059	0.078	-0.132	0.030	-0.131	0.215	0.047	-0.160
	NO	0.257	-0.068	-0.325	-0.003	0.139	0.127	-0.143	0.062	0.088	-0.133	0.045	-0.160	0.215	0.048	-0.149
Cl	CH	0.268	-0.118	-0.347	-0.025	0.222	0.064	-0.065	0.061	0.029	-0.090	0.014	-0.093	0.218	0.045	-0.184
	H	0.266	-0.109	-0.344	-0.022	0.208	0.069	-0.075	0.059	0.031	-0.084	0.018	-0.104	0.215	0.043	-0.172
	F	0.268	-0.114	-0.342	-0.020	0.208	0.069	-0.077	0.060	0.033	-0.086	0.017	-0.099	0.218	0.044	-0.179
	Cl	0.266	-0.106	-0.340	-0.019	0.200	0.073	-0.081	0.059	0.038	-0.089	0.021	-0.109	0.216	0.045	-0.173
	CN	0.260	-0.088	-0.332	-0.013	0.173	0.113	-0.115	0.059	0.073	-0.130	0.033	-0.133	0.214	0.045	-0.160
	NO	0.255	-0.069	-0.323	-0.004	0.140	0.128	-0.142	0.062	0.084	-0.132	0.047	-0.160	0.214	0.047	-0.148
CN	CH	0.267	-0.123	-0.345	-0.034	0.234	0.061	-0.049	0.067	0.012	-0.091	0.022	-0.095	0.221	0.041	-0.189
	H	0.265	-0.113	-0.341	-0.031	0.219	0.065	-0.061	0.064	0.015	-0.083	0.026	-0.107	0.218	0.039	-0.177
	F	0.267	-0.119	-0.339	-0.029	0.220	0.066	-0.061	0.066	0.017	-0.088	0.024	-0.101	0.220	0.041	-0.185
	Cl	0.265	-0.111	-0.337	-0.028	0.211	0.069	-0.067	0.064	0.020	-0.086	0.028	-0.111	0.219	0.041	-0.178
	CN	0.259	-0.092	-0.329	-0.022	0.184	0.091	-0.091	0.062	0.040	-0.102	0.039	-0.135	0.216	0.043	-0.163
	NO	0.254	-0.073	-0.320	-0.013	0.151	0.128	-0.132	0.065	0.069	-0.130	0.052	-0.160	0.215	0.044	-0.151
NO	CH	0.268	-0.130	-0.342	-0.049	0.253	0.055	-0.024	0.076	-0.010	-0.097	0.033	-0.097	0.227	0.034	-0.197
	H	0.265	-0.119	-0.337	-0.046	0.237	0.059	-0.036	0.072	-0.009	-0.087	0.036	-0.109	0.224	0.033	-0.184
	F	0.268	-0.126	-0.336	-0.044	0.238	0.059	-0.035	0.074	-0.006	-0.092	0.035	-0.104	0.226	0.033	-0.191
	Cl	0.265	-0.117	-0.334	-0.043	0.229	0.062	-0.042	0.072	-0.003	-0.089	0.038	-0.112	0.225	0.034	-0.184
	CN	0.259	-0.098	-0.325	-0.037	0.201	0.075	-0.065	0.068	0.008	-0.085	0.047	-0.136	0.221	0.037	-0.169
	NO	0.254	-0.078	-0.315	-0.028	0.167	0.125	-0.114	0.069	0.048	-0.128	0.058	-0.161	0.219	0.039	-0.154

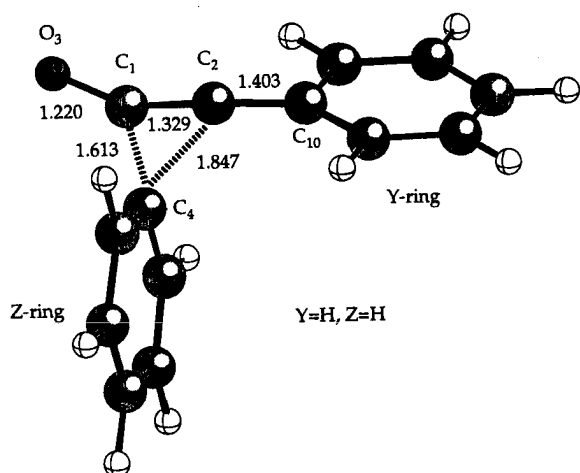
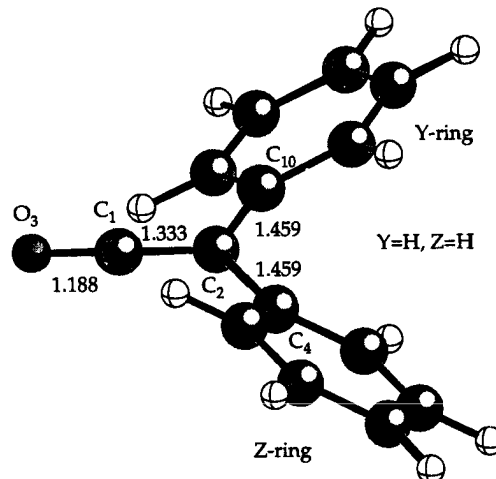
**Figure 2.** Structure of transition state (TS). Y: H, Z: H. Bond lengths in Å.**Figure 3.** Structure of product (P). Y: H, Z: H. Bond lengths in Å.

Table 3. Heats of formation, ΔH_f , entropies, S , Gibbs free energies of reaction, ΔG° and of activation, ΔG^\ddagger , in kcal mol $^{-1}$

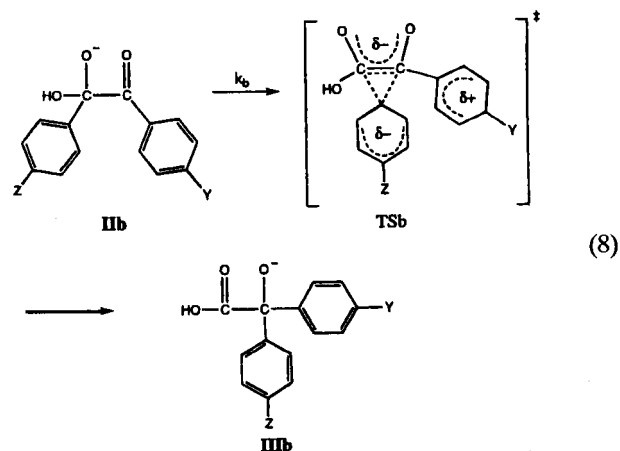
Z	Y	ΔH_f			S			ΔG°	ΔG^\ddagger
		reactant	TS	product	reactant	TS	product		
CH ₃	CH ₃	85.49	107.30	30.88	133.39	132.18	131.89	-54.61	22.17
	H	93.89	115.15	38.56	124.54	123.07	121.69	-55.33	21.70
	F	48.48	69.86	-6.62	127.48	126.62	125.94	-55.11	21.64
	Cl	87.43	108.09	31.40	130.12	131.08	127.48	-56.03	20.37
	CN	127.96	146.15	69.86	132.37	131.93	129.15	-58.11	18.31
	NO ₂	102.23	117.10	41.54	139.45	135.91	135.53	-60.70	15.92
H	CH ₃	93.21	115.40	38.55	123.51	123.52	120.97	-54.66	22.19
	H	101.62	123.25	46.23	113.18	111.89	110.02	-55.39	22.01
	F	56.23	78.00	1.07	117.29	116.09	114.38	-55.16	22.12
	Cl	95.18	116.25	39.10	120.07	119.04	117.56	-56.08	21.38
	CN	135.74	154.51	77.58	122.12	122.11	119.34	-58.16	18.78
	NO ₂	110.06	125.58	49.30	129.19	126.12	125.53	-60.76	16.44
F	CH ₃	47.78	70.12	-6.62	127.57	127.89	124.88	-54.40	22.25
	H	56.24	78.01	1.07	117.25	115.99	114.80	-55.16	22.14
	F	10.91	32.83	-43.98	121.40	120.12	118.52	-54.88	22.31
	Cl	49.86	71.12	-5.96	124.25	123.03	121.84	-55.82	21.62
	CN	90.53	109.68	32.63	126.17	126.27	123.79	-57.89	19.12
	NO ₂	64.99	80.87	4.51	133.03	130.41	129.80	-60.48	16.66
Cl	CH ₃	86.06	108.72	31.40	130.11	128.91	127.79	-54.66	23.02
	H	94.52	116.62	39.10	120.02	118.64	117.01	-55.42	22.52
	F	49.18	71.45	-5.96	124.07	122.81	121.12	-55.14	22.64
	Cl	88.14	109.75	32.07	126.94	125.64	123.75	-56.07	21.99
	CN	128.81	148.37	70.68	128.93	129.10	126.20	-58.13	19.51
	NO ₂	103.28	119.57	42.58	135.73	133.27	132.23	-60.70	17.02
CN	CH ₃	124.89	148.42	69.86	131.90	130.51	128.47	-55.03	23.95
	H	133.40	156.39	77.58	121.76	120.47	118.92	-55.82	23.37
	F	88.13	111.31	32.63	125.89	124.57	122.94	-55.49	23.58
	Cl	127.09	149.66	70.67	128.68	127.37	125.71	-56.41	22.96
	CN	167.88	188.83	109.44	130.66	129.82	127.77	-58.44	21.19
	NO ₂	142.52	160.33	81.56	137.24	135.42	133.36	-60.96	18.36
NO ₂	CH ₃	97.00	121.55	41.54	137.73	136.48	136.13	-55.46	24.93
	H	105.60	129.60	49.30	127.63	126.40	125.60	-56.30	24.37
	F	60.41	84.68	4.51	131.79	130.63	130.10	-55.90	24.62
	Cl	99.39	123.08	42.57	134.60	133.26	132.21	-56.81	24.09
	CN	140.36	162.69	81.56	136.56	135.26	133.40	-58.79	22.72
	NO ₂	115.25	135.08	54.01	143.14	142.39	138.90	-61.24	20.06

Table 4. The Hammett's ρ_z and ρ_y values and cross-interaction constant, ρ_{zy}

Z:Y	ρ_z	ρ_y
CH ₃	-2.127 (0.968)	2.931 (0.974)
H	-1.883 (0.974)	3.045 (0.980)
F	-2.060 (0.978)	2.838 (0.966)
Cl	-2.442 (0.974)	2.930 (0.974)
CN	-3.165 (0.977)	2.574 (0.951)
NO ₂	-2.845 (0.962)	2.184 (0.937)
multiple regression		$\rho_z = -1.399$ $\rho_y = 2.955$ $\rho_{zy} = -0.525 (0.941)$

^acorrelation coefficient values are shown in parentheses.

of 4,4'-disubstituted benzils (IIb) in the gas phase, eq. 8.¹⁴ For the benzilic rearrangement step, k_b , the multiple regression of the $\delta\Delta G^\ddagger$ data using eq. 3 gave the cross-



interaction constant $r_{yz} = -0.48$ as expressed in eq. 9.¹⁴ In this

$$\log(k_{zy}^{\ddagger}/k_{zz}^{\ddagger}) = -1.76\sigma_z + 3.83\sigma_y - 0.48\sigma_z\sigma_y \quad (9)$$

rearrangement, large electronic charge is carried by the Z-ring in the TS. The electronic charge in the TS partially comes from the C₁-moiety, and as a result the Z-ring is negatively charged and the C₂-moiety becomes positively charged in the TS. This is in quite contrast to those found in this work. For the benzylic rearrangement, eq. 8, the interaction between the two rings increases in the TS (relatively large magnitude of ρ_{1z} ($= -0.48$)), but in the rearrangement of the azibenzil (the magnitude of ρ_{1z} ($= -0.53$)) is slightly larger. Since the magnitude of ρ_{1z} represents the change in the intensity of interaction between the two substituents on going from the initial (IIa or IIb) to the TS (TSa or TSb),¹⁶ eq. 5, the slightly greater magnitude of ρ_{1z} in the change from IIa to TSa as compared to that in the change from IIb to TSb may be ascribed to slightly greater increase of interaction: the relatively stable initial state in IIa due to the vicinal n- σ^* overlap could increase ΔI_{1z} and hence the magnitude of ρ_{1z} in eq. 5 for the azibenzil rearrangement. In both cases, *i.e.*, in TSa and TSb, the bridged TS structure causes considerable increase in the interaction between Y and Z.

Solvent Effects

Since the SM2.1 model of the Cramer and Truhlar method is a quantum statistical continuum-dielectric model, there is very little changes in the reactants, TSs and products structurally. In fact, we have shown that single point calculations on the energies and the Hammett coefficients ρ_1 and ρ_2 using the gas-phase geometries (SM2.1/AM1//AM1) for the identity S_N2 reactions of (Y)-benzyl chlorides with Cl⁻ anion differ (<5%) very little from the corresponding values calculated by full optimization (SM2.1/AM1//SM2.1/AM1).¹⁷ Thus, in this work, we carried out single point calculations.

The solvation energies, ΔG_{solv} , and the activation energies in water, $\Delta G^\ddagger + \Delta G_{\text{solv}}$, are summarized in Table 5. The activation energies in water obtained in this way are used to derive various selectivity parameters, ρ_{1z} , ρ_{2z} and ρ_{12z} , by eqs. 6 and 3. The results are collected in Table 6. By comparison, all the ρ_{1z} and ρ_{2z} values have greater magnitude in aqueous solution. This is reasonable, since in this reaction charges are dispersed in the TS from the charge separated reactant, IIa', so that the solvent water stabilizes the reactant more than the transition state. In addition, there is a reversal of charge on going from the reactant (negative charge on the Z-ring and positive charge on the Y-ring) to the TS (positive charge on the Z-ring and negative charge on the Y-ring), Table 2, leading to a relatively large change in the solvation energy and hence to the greater magnitude of the ρ values. In accordance with this reversal of charge accompanied by a large structural change in water, the cross interaction between the substituents Y and Z, ρ_{12z} , also increases with a larger magnitude of ρ_{12z} ($= -0.66$) in water. This is, however, in contrast with the solvent effects found for the benzylic rearrangement, in which negative charge (-1) is dispersed but without a reversal of charge in the TS. In the benzylic rearrangement, we found that the cross interaction between Y and Z decreased in water, to approximately by half.

We conclude that the Wolff rearrangements of α -keto-carbenes involve a charge-transferred bridged TS (TSa)

Table 5. The solvation free energies (in kcal/mol) and sum of the activation and solvation free energies (in kcal/mol) in aqueous solution

Z	Y	ΔG_{solv}	$\Delta G^\ddagger + \Delta G_{\text{solv}}$
CH ₃	CH ₃	2.39	24.56
	H	2.27	23.98
	F	1.78	23.41
	Cl	1.96	22.33
	CN	1.14	19.45
	NO ₂	0.77	16.69
	H	CH ₃	2.44
H		2.34	24.35
F		1.85	23.97
Cl		2.02	23.40
CN		1.18	19.96
NO ₂		0.83	17.27
F		CH ₃	2.53
	H	2.44	24.58
	F	1.96	24.27
	Cl	2.12	23.74
	CN	1.38	20.50
	NO ₂	1.06	17.72
	Cl	CH ₃	2.57
H		2.46	24.98
F		2.01	24.64
Cl		2.16	24.16
CN		1.45	20.96
NO ₂		1.15	18.17
CN		CH ₃	2.75
	H	2.66	26.03
	F	2.23	25.81
	Cl	2.35	25.32
	CN	1.88	23.07
	NO ₂	1.55	19.90
	NO ₂	CH ₃	2.72
H		2.60	26.97
F		2.17	26.79
Cl		2.26	26.35
CN		1.70	24.42
NO		1.41	21.47

Table 6. The Hammett's ρ_{1z} and ρ_{2z} values and cross-interaction constant, ρ_{12z} in aqueous solution

Z:Y	ρ_{1z}	ρ_{2z}
CH ₃	-2.398 (0.979)	3.727 (0.984)
H	-2.162 (0.985)	3.840 (0.987)
F	-2.503 (0.983)	3.557 (0.979)
Cl	-2.704 (0.982)	3.619 (0.983)
CN	-3.697 (0.988)	3.133 (0.963)
NO	-3.407 (0.981)	2.804 (0.959)
	multiple regression	$\rho_{1z} = -1.566$ $\rho_{2z} = 3.752$ $\rho_{12z} = -0.661 (0.937)$

*correlation coefficient values are shown in parentheses.

from the migrating ring (Z-ring) toward the nonmigrating ring (Y-ring). However due to the relatively strong in-

teraction caused by the vicinal n- σ^* overlap in the initial state (IIa), the initial state is relatively stabilized. Moreover there occurs a complete reversal in the effects of substituents Y and Z from the initial to transition state, which will no doubt brings a relatively large structural change on going from the initial to the transition state. Thus there is relatively larger increase in the interaction between the two substituents, Y and Z, in the TS and hence results in a relatively larger magnitude of ρ_{yz} ($= -0.53$) compared to that for the similar step in the base-catalyzed benzylic rearrangement ($\rho_{yz} = -0.48$); for the latter no such initial state interaction exists and results in a relatively smaller increase in the interaction in the TS with a larger magnitude of ρ_{yz} . Charge dispersal in the TS leads to an increase in ρ_x , ρ_y and ρ_z values in water.

Acknowledgment. We thank Inha University for support of this work. One of authors (C. K. Kim) also thanks the Korea Science and Engineering Foundation (961-0305-046-2) for support of this work.

References

1. Wolff, L. *Ann.* **1902**, 325, 129.
2. (a) Wolff, L. *Ann.* **1912**, 394, 23. (b) Staudinger, H.; Hürzel, H. *Ber. Deut. Chem. Ges.* **1916**, 49, 2522. (c) Gilman, H.; Adams, Ch. E. *Rec. Trav. Chim.* **1929**, 48, 464. (d) Georgian, V.; Boyer, S. K.; Edwards, B. *J. Org. Chem.* **1980**, 45, 1686. (e) Tomioka, H.; Hayashi, N.; Asano, T.; Izawa, Y. *Bull. Chem. Soc. Japan*, **1983**, 56, 758.
3. Schroeter, G. *Ber. Deut. Chem. Ges.* **1909**, 42, 3356.
4. Kirmse, W. *Carbene Chemistry*; Academic Press: New York, U. S.A., 1964; p 118.
5. (a) Lee, I. *Chem. Soc. Rev.* **1990**, 19, 317. (b) Lee, I. *Adv. Phys. Org. Chem.* **1992**, 27, 57. (c) Lee, I. *Chem. Soc. Rev.* **1995**, 24, 223.
6. Lee, I. *J. Phys. Org. Chem.* **1992**, 5, 736.
7. (a) Dewar, M. J. S.; Zochisch, E. G.; Healy, F. P.; Stewart, J. J. P. *J. Am. Chem. Soc.* **1985**, 107, 3902. (b) MOPAC 6.0 program, available from Quantum Chemistry Program Exchange (QCPE) No. 506.
8. Csizmadia, I. G. *Theory and Practice of MO Calculations on Organic Molecules*; Elsevier: Amsterdam, 1976; p 239.
9. (a) Liotard, D. A.; Howkins, G. D.; Lynch, G. C.; Cramer, C. J.; Truhlar, D. G. *J. Comput. Chem.* **1995**, 16, 422. (b) Cramer, C. J.; Truhlar, D. G. *J. Am. Chem. Soc.* **1991**, 113, 8305. (c) Cramer, C. J.; Truhlar, D. G. *J. Comput. Chem.* **1992**, 13, 1089. (d) Cramer, C. J.; Truhlar, D. G. *J. Am. Chem. Soc.* **1994**, 116, 3892. (e) Giesen, D. J.; Storer, J. W.; Cramer, C. J.; Truhlar, D. G. *J. Am. Chem. Soc.* **1995**, 117, 1057. (f) AMSOL 5.0 program, available, from Quantum Chemistry Program Exchange (QCPE) No. 606.
10. Storer, J. W.; Giesen, D. J.; Howkins, G. D.; Lynch, G. C.; Cramer, C. J.; Truhlar, D. G.; Liotard, D. A. *Structure and Reactivity in Aqueous Solution. Characterization of Chemical and Biological Systems*; Cramer, C. J., Truhlar, D. G. Ed.; American Chemical Society: Washington D.C., 1994; chapter 3.
11. (a) Brunck, T. K.; Weinhold, F. *J. Am. Chem. Soc.* **1979**, 101, 1700. (b) Weinhold, F.; Brunck, T. K. *J. Am. Chem. Soc.* **1976**, 98, 3745. (c) Brunck, T. K.; Weinhold, F. *J. Am. Chem. Soc.* **1976**, 98, 4392. (d) Lee, I.; Cheun, Y. G.; Yang, K. *J. Comput. Chem.* **1982**, 3, 565.
12. Sutton, L. E. Ed. *Tables of Interatomic Distances and Configurations in Molecules and Ions Special Publication No. 11*, The Chem. Soc., London, 1958.
13. Exner, O. *Correlation Analysis in Chemistry*; Plenum Press: New York, 1978, chapter 10.
14. Lee, I.; Lee, D.; Lee, J. K.; Kim, C. K.; Lee, B.-S. *J. Chem. Soc. Perkin Trans 2*, **1996**, 2519.
15. Lee, I.; Kim, C. K.; Lee, B.-S.; Kim, C. K.; Lee, H. W.; Han, I. S. *J. Phys. Org. Chem.* submitted for publication, 1996.